Supporting information

Copper Nanoparticles Dotted on Copper Sulfide Nanosheets for Selective Electrocatalytic Oxidation of Glycerol to Formate

Jiawei Du [a], Yang Qin [a,b], Tong Dou [a], Jingmin Ge [a], Yiping Wang [a,*], Xuhui Zhao[a], Fazhi Zhang [a], Xiaodong Lei [a,*]

[a] State Key Laboratory of Chemical Resource Engineering, Beijing University of Chemical Technology, Beijing 100029, China

[b] Advanced Technology Department, RiseSun MGL, Inc. Beijing 102299, China

* Corresponding author

Tel.: +86-10-64455357; Fax: +86-10-64425385

E-mail: wangyiping@buct.edu.cn (Yiping Wang)

leixd@mail.buct.edu.cn (Xiaodong Lei)

Number of pages: 10

Number of tables: 3

Number of figures: 7

Electronic Supplementary Information Index

Table S1. The values of C_{dl} and ECSA of the electrodes.

Table S2. Comparison of GOR performance and products of Cu-CuS/BM with reported non-noble metal electrocatalysts.

Table S3. The adsorption energy of GLY molecule on the different lattice planes.

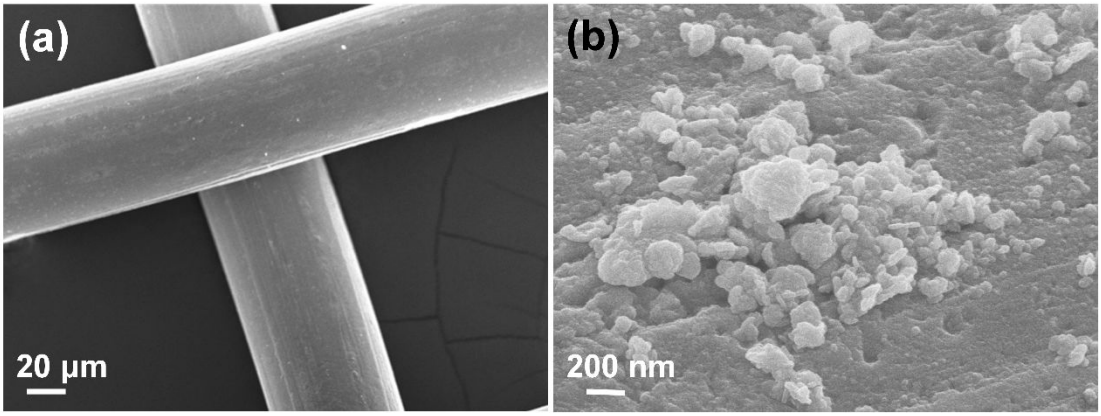

Figure S1. SEM images of the (a) BM and (b) Cu-BM.

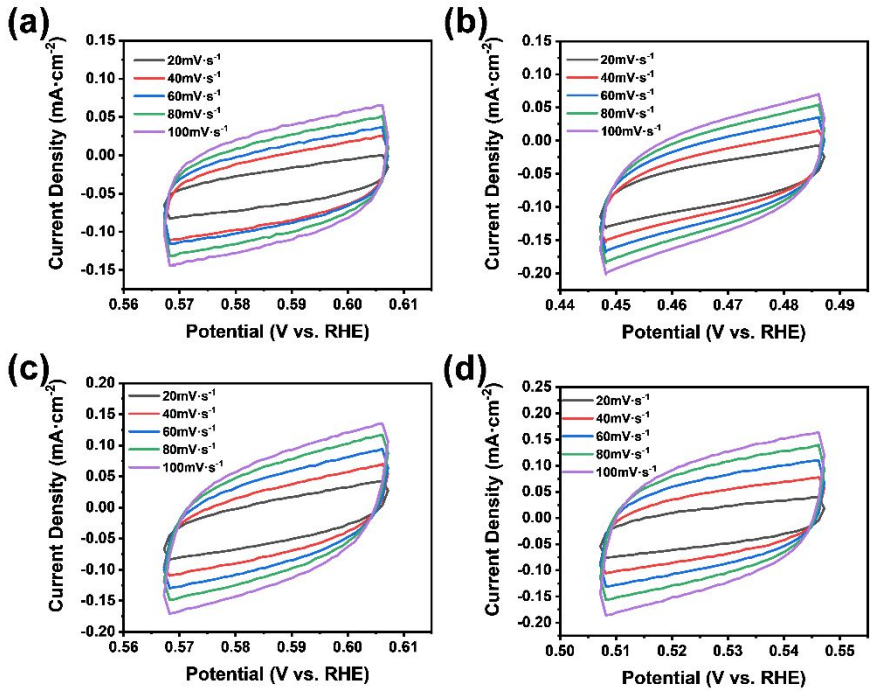

Figure S2. CV curves of the (a) BM, (b) CuS/BM, (c) Cu-BM and (d) Cu-CuS/BM at various scan rates in 0.1 M KOH in the presence of 0.1 M GLY.

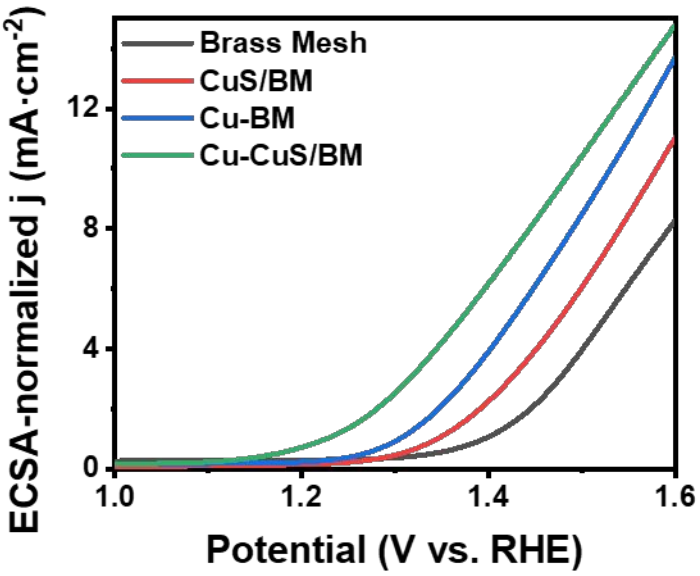

Figure S3. ECSA-normalized LSV curves of Brass Mesh, CuS/BM, Cu-BM and Cu-CuS/BM for GOR in 0.1 M KOH solution with 0.1 M glycerol.

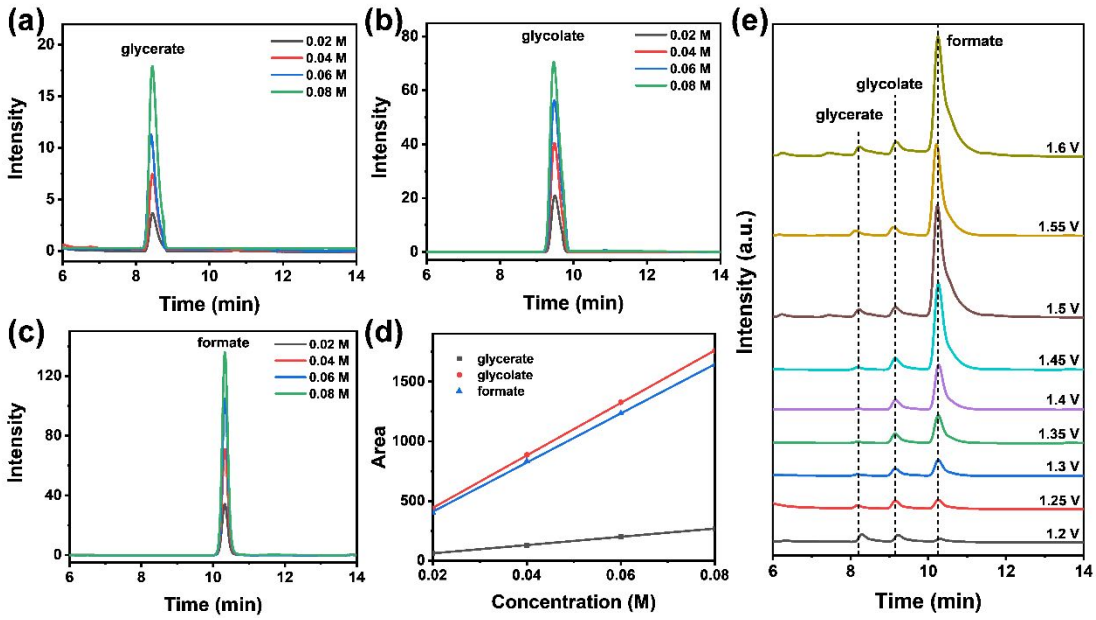

Figure S4. Standard HPLC chromatograms of glycerate (a), glycolate (b) and formate (c). (d) The standard curves of glycerate, glycolate and formate. (e) HPLC chromatograms of the reaction products from the GOR at different potentials using Cu-CuS/BM.

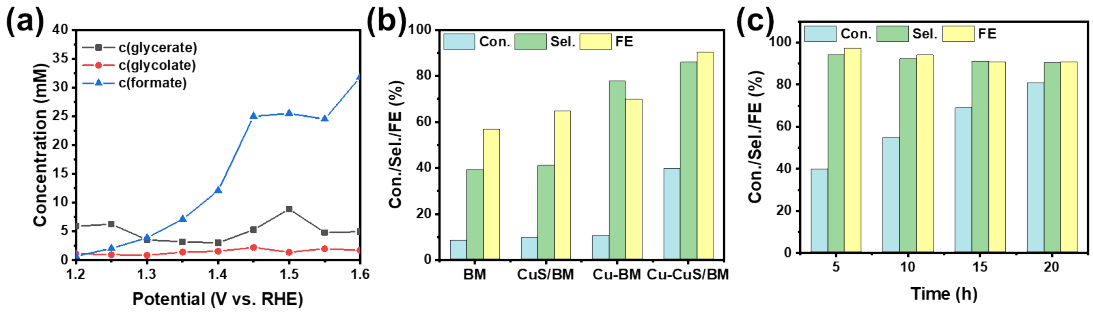

Figure S5. (a) The concentrations of the all products for GOR detected by HPLC, including glycerate, glycolate and formate. (b) The Conversion of GLY, the Selectivity and Faradaic efficiency of formate at the 1.45 V vs. RHE for GOR using the BM, CuS/BM, Cu-BM, Cu-CuS/BM. (c) The Conversion of GLY, the Selectivity and Faradaic efficiency of formate on Cu-CuS/BM after reacting 5 h, 10 h, 15 h and 20 h.

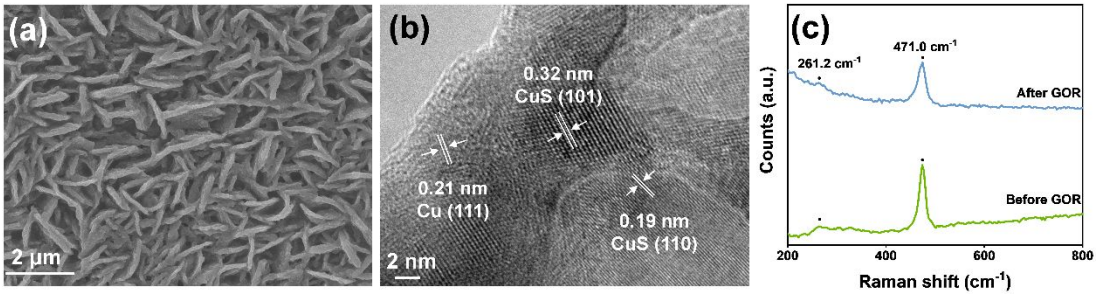

Figure S6. The SEM (a) and HRTEM (b) images of Cu-CuS/BM after long-term electrolysis. (c) The Raman spectra of Cu-CuS/BM before and after electrochemical test.

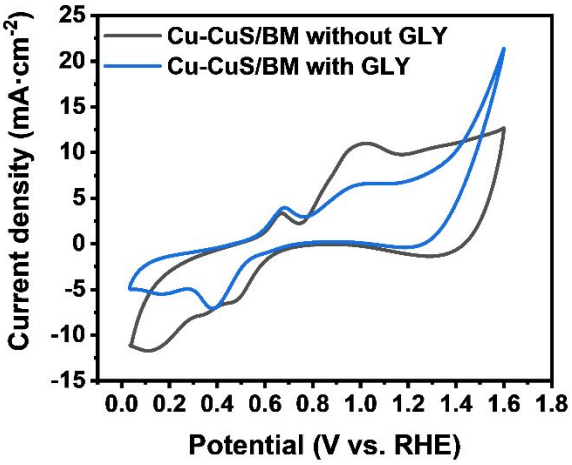

Figure S7. CV curves of the Cu-CuS/BM in 0.1 M KOH with and without 0.1 M GLY.

Table S1. The values of C_{dl} and ECSA of the electrodes.

Catalyst	C_{dl} (mF·cm^{-2})	ECSA
Brass Mesh	1.28	1
CuS/BM	1.34	1.05
Cu-BM	1.74	1.36
Cu-CuS/BM	2.46	1.92

The ECSA for Brass Mesh was defined to be 1, and the geometric area of all catalysts were 1 cm^2.[1-2]

Table S2. Comparison of GOR performance and products of Cu-CuS/BM with reported non-noble metal electrocatalysts.

Catalysts	pH	Potential at 10 $mA \cdot cm^{-1}$ (V vs RHE)	Main product	Potential at Sel_{max} (V vs RHE)	Sel. (%)	Ref
Cu-CuS/BM	13	1.37 V	formate	1.45	86.0	**This work**
$CuCo_2O_4$	13	1.26 V	formate	1.30	80.6	3
CuO	13	-	formate	1.27 1.69	70.0 98.0	4
Cu_1Ni_1@ACF	13	-	formate	1.665	97.4	5
Ni/C CoNi/C FeNi/C FeCoNi/C	13	-	formate	1.60	32.2 7.5 4.0 34.1	6
Nickel-molybdenum nitride Ni	14	1.30 V	formate	1.35	92.5 48.1	7
$Ni_{90}Bi_{10}$ $Ni_{90}Bi_{10\text{-aging-2w}}$	14	-	formate	1.55	38.6 25.4	8
Ni_xM_{1-x}/C (M=Pd,Au, and Bi)	14	-	formate	1.55	100	9
Poly[Ni(salen)] film	14	-	formate glycolate	-	-	10

Ni/Cu	14	1.43 V	oxalate	-	-	11

Table S3. The adsorption energy of GLY molecule on the different lattice planes.

Sub	E_{tot}/eV	E_{sub}/eV	E_{GLY}/eV	E_{ad}/eV
Cu (111)	-107784.82	-105875.45	-1918.93	9.55
CuS (101)	-29689.74	-27770.78	-1918.95	-0.02
CuS (110)	-37633.54	-35714.78	-1918.98	0.22
Cu (111)-CuS	-143493.86	-141570.80	-1918.96	-4.10

REFERENCES

1. Lei, Q.; Zhu, H.; Song, K.; Wei, N.; Liu, L.; Zhang, D.; Yin, J.; Dong, X.; Yao, K.; Wang, N.; Li, X.; Davaasuren, B.; Wang, J.; Han, Y., Investigating the origin of enhanced C_{2+} selectivity in oxide-/hydroxide-derived copper electrodes during CO_2 electroreduction. *J. Am. Chem. Soc.* **2020,** *142* (9), 4213-4222, DOI 10.1021/jacs.9b11790.
2. Dou, T.; Qin, Y.; Zhang, F.; Lei, X., CuS nanosheet arrays for electrochemical CO_2 reduction with surface reconstruction and the effect on selective formation of formate. *ACS Appl. Energ. Mater.* **2021,** *4* (5), 4376-4384, DOI 10.1021/acsaem.0c03190.
3. Han, X.; Sheng, H.; Yu, C.; Walker, T. W.; Huber, G. W.; Qiu, J.; Jin, S., Electrocatalytic oxidation of glycerol to formic acid by $CuCo_2O_4$ spinel oxide nanostructure catalysts. *ACS Catal.* **2020,** *10* (12), 6741-6752, DOI 10.1021/acscatal.0c01498.
4. Liu, C.; Hirohara, M.; Maekawa, T.; Chang, R.; Hayashi, T.; Chiang, C.-Y., Selective electro-oxidation of glycerol to dihydroxyacetone by a non-precious electrocatalyst – CuO. *Appl. Catal. B* **2020,** *265*, 118543, DOI 10.1016/j.apcatb.2019.118543.
5. Zhang, J.; Shen, Y., Electro-oxidation of glycerol into formic acid by nickel-copper electrocatalysts. *J. Electrochem. Soc.* **2021,** *168* (8), 084510, DOI 10.1149/1945-7111/ac1cfd.
6. Oliveira, V. L.; Morais, C.; Servat, K.; Napporn, T. W.; Tremiliosi-Filho, G.; Kokoh, K. B., Studies of the reaction products resulted from glycerol electrooxidation on Ni-based materials in alkaline medium. *Electrochim. Acta* **2014,** *117*, 255-262, DOI 10.1016/j.electacta.2013.11.127.
7. Li, Y.; Wei, X.; Chen, L.; Shi, J.; He, M., Nickel-molybdenum nitride nanoplate electrocatalysts for concurrent electrolytic hydrogen and formate productions. *Nat. Commun.* **2019,** *10* (1), 5335, DOI 10.1038/s41467-019-13375-z.
8. Houache, M. S. E.; Hughes, K.; Safari, R.; Botton, G. A.; Baranova, E. A., Modification of nickel surfaces by bismuth: effect on electrochemical activity and selectivity toward glycerol. *ACS Appl. Mater. Inter.* **2020,** *12* (13), 15095-15107, DOI 10.1021/acsami.9b22378.
9. Houache, M. S. E.; Safari, R.; Nwabara, U. O.; Rafaïdeen, T.; Botton, G. A.; Kenis, P. J. A.; Baranton, S.; Coutanceau, C.; Baranova, E. A., Selective electrooxidation of glycerol to formic acid over carbon supported $Ni_{1-x}M_x$ (M = Bi, Pd, and Au) nanocatalysts and coelectrolysis of CO_2. *ACS Appl. Energ. Mater.* **2020,** *3* (9), 8725-8738, DOI 10.1021/acsaem.0c01282.
10. Bott-Neto, J. L.; Martins, T. S.; Machado, S. A. S.; Ticianelli, E. A., Electrocatalytic oxidation of methanol, ethanol, and glycerol on $Ni(OH)_2$ nanoparticles encapsulated with poly[Ni(salen)] film. *ACS Appl. Mater. Inter.* **2019,** *11* (34), 30810-30818, DOI 10.1021/acsami.9b08441.
11. Rizk, M. R.; Abd El-Moghny, M. G.; Mazhar, A.; El-Deab, M. S.; El-Anadouli, B. E., Dual-functioning porous catalysts: robust electro-oxidation of small organic molecules and water electrolysis using bimetallic Ni/Cu foams. *Sustain. Energ. Fuels* **2021,** *5* (4), 986-994, DOI 10.1039/d0se01835j.